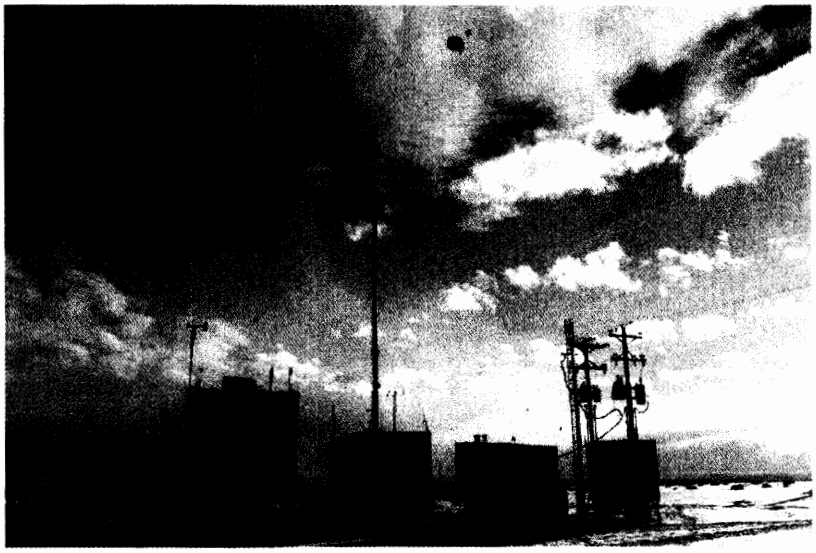

Final Report
2013 Uinta Basin Winter Ozone Study

Prepared for:
Brock LeBaron
Utah Division of Air Quality
1950 West 150 North
Salt Lake City, UT 84116

Edited by:
Till Stoeckenius
ENVIRON International Corporation
and
Dennis McNally
Alpine Geophysics

ENVIRON International Corporation
773 San Marin Drive, Suite 2115
Novato, California, 94998
www.environcorp.com
P-415-899-0700
F-415-899-0707

March 2014

ENVIRON

Due to the large volume of the Final Report on the 2013 Uintah Basin Winter Ozone study, EPA is providing in the hardcopy Administrative Record only the excerpts from the Report that are cited in section #G.3 of EPA's Response to Comments on the draft title V permit for the Deseret Bonanza power plant. The full report is available electronically from EPA.

EXECUTIVE SUMMARY

Background

The Uinta Basin is a rural area of northeastern Utah where the majority of the state's oil and gas production occurs. Ozone concentrations in excess of the current national air quality standard have been measured in the Basin during the winter. These high ozone levels are only observed in the Basin during winter inversion periods when the ground is covered by snow; ozone levels outside of these periods have remained below the air quality standard and conditions resulting in exceedances of the standard do not occur every year.

In the first quarter of 2012, a multi-phased study (the Uinta Basin Ozone Study, UBOS) was begun to identify the emissions sources and the unique photochemical processes that cause elevated winter ozone concentrations, and to identify the most effective strategies to reduce winter ozone. UBOS 2012 included measurements of ozone and ozone precursor concentrations and meteorological conditions throughout the Basin. Meteorological conditions during UBOS 2012 were not conducive to ozone formation due to a lack of snow cover; no exceedances of the 8-hour average 75 parts per billion (ppb) National Ambient Air Quality Standard (NAAQS) were observed during UBOS 2012. Key findings from UBOS 2012 are described in a summary report (Final Report: 2012 Uinta Basin Winter Ozone and Air Quality Study; available at http://www.deq.utah.gov/locations/uintahbasin/studies/2012study.htm.)

UBOS 2013 took place between January and March 2013. In contrast to UBOS 2012, conditions during UBOS 2013 were favorable to ozone formation and numerous exceedances of the NAAQS were observed. Results from UBOS 2013, in combination with those from UBOS 2012, provide a wealth of information about the meteorological conditions and atmospheric chemistry associated with winter ozone episodes in the Uinta Basin.

This important work is made possible by funding and in-kind support from the following: Uintah Impact Mitigation Special Service District (UIMSSD), Western Energy Alliance, Questar Energy Products, Bureau of Land Management (BLM), National Oceanic and Atmospheric Administration (NOAA), Environmental Protection Agency (EPA), Utah Department of Environmental Quality (UDEQ), Utah Science Technology and Research Initiative (USTAR), and Utah School and Institutional Trust Lands Administration (SITLA). Work on UBOS 2013 was conducted by researchers from Utah State University (USU); National Oceanic and Atmospheric Administration (NOAA); Utah Department of Environmental Quality (UDEQ); University of Utah (UU); University of Colorado, Boulder (CU); University of Wyoming (U of WY); University of California Los Angeles (UCLA); and University of Washington (UW).

Findings

Key findings from UBOS 2013 are summarized below:

I. Air Quality
   a. Maximum 8-hour average ozone concentrations measured at Ouray, which typically has among the highest readings in the Basin, reached 142 ppb during the December 2012 – March 2013 winter study, exceeding the EPA 8-hour

standard (75 ppb) by 89%. Exceedances of the standard (i.e., a daily maximum 8-hour average in excess of 75 ppb) occurred at 17 of the 20 monitoring sites operating during the study. Monitors in the major Basin population centers exceeded the standard on a total of 22 days at Vernal and 29 days at Roosevelt during 2013 with all of the exceedances occurring between January 9th and March 6th. Note that the occurrence of an exceedance does not by itself constitute a *violation* of the EPA standard; a violation only occurs when the three year average of the annual fourth highest daily maximum 8-hour average is greater than 75 ppb. Exceedances occurred in the Basin during seven separate multi-day ozone episodes which were separated by periods of lower ozone levels coinciding with the passage of storm systems. These observations are in sharp contrast to conditions during the 2011-2012 winter study, when daytime 8-hour average ozone levels did not exceed 63 ppb.

b. Individual ozone episodes ranged from 3 to nearly 15 days in length, with ozone concentrations generally increasing from one day to the next during each episode, indicating a lack of ventilation.
c. Daytime ozone concentrations at locations close to but outside of the Uinta Basin, at the time of high surface ozone events inside the basin, ranged from 40 to 60 ppb. Ozone concentrations measured inside the Basin above the temperature inversion during these periods were also in the 40 to 60 ppb range. These facts, combined with observations of winds around the Basin, confirms that high surface ozone concentrations within the basin are not influenced to any significant extent by transport of ozone or precursors from outside of the Basin.
d. Days with high ozone in the Basin coincide with elevated levels of methane, volatile organic compounds (VOC) and odd nitrogen species (NO_y). Alkane hydrocarbons constitute the main fraction of identified VOC. VOC and NO_x are the primary chemical precursors of ozone. A review of all emissions sources within the Basin (based on WRAP Phase III and UDAQ triennial inventories) indicates that activities associated with oil and gas exploration and production are the predominant sources of ozone precursors.
e. VOC concentrations in the Basin are extremely high during ozone episodes due to large amounts of VOC emissions and limited ventilation under a strong temperature inversion. Average VOC levels at Horsepool in 2013 were 1,684 ppbC (based on C2 – C7 non-methane hydrocarbons) as compared to 232 ppbC in 2012 when inversions were not present and there was more mixing.
f. Vertical profiles show that the polluted air mass associated with ozone episodes is confined to a shallow boundary layer that varies in height from 70 – 400 m (230 – 1,300 ft) above ground level.
g. The Bonanza power plant plume does not appear to contribute any significant amount of nitrogen oxides or other contaminants to the polluted boundary layer during ozone episodes; the thermally buoyant Bonanza plume was observed to rise upwards from the 183 m (600 ft) stack and penetrates through the temperature inversion layer. As a result, emissions from the Bonanza plant are

effectively isolated from the boundary layer in which the high ozone concentrations occur.

II. Meteorology

a. Observations made during the 2013 winter study confirmed that high winter ozone in the Uinta basin only occurs when the ground is covered with snow and weather conditions promote the formation of a strong temperature inversion which traps a layer of cold, stable air (a "cold pool") within the basin. In the absence of any snow cover, warming of the earth's surface by the sun causes too much convective mixing for a cold pool to form.

b. Chemical reactions resulting in ozone formation are driven by the illumination of the atmosphere from direct, reflected and scattered ultraviolet solar radiation. Reflection of light from the snow surface significantly increases (by roughly 50%) the total flux of ultraviolet radiation and thus the rate of ozone formation.

c. Ozone episodes in the Basin are characterized by complex, diurnally varying patterns of light winds which have the potential to produce gradual but significant intra-basin transport of ozone and precursors. Factors driving winds within the polluted boundary layer include differential daytime heating producing upslope flows (which can be modified by variations in snow cover), nighttime drainage flows resulting in convergence along the river valleys at the lowest Basin elevations, and spatial perturbations of the depth of the cold pool air mass by winds blowing over the mountains surrounding the Basin. These forcing factors appear to produce oscillations or an east-west "sloshing" of air within the basin that further contributes to intra-basin mixing. These processes result in transport of ozone and ozone precursors from one part of the Basin to another but are not strong enough to mechanically breakdown the temperature inversion.

d. Initial attempts at modeling meteorological conditions during episodes indicate that obtaining accurate results with current modeling techniques will be very challenging. Additional data collection and model development and testing will be required to produce a good working model suitable for evaluating alternative regulatory strategies.

III. Chemistry

a. Unique features of the chemical reactions involved in ozone production were observed during the 2013 winter ozone episodes which make these episodes very different from summer ozone episodes in urban areas. Nitrous acid (HONO) and formaldehyde rather than ozone photolysis were found to be the biggest contributors to the pool of chemical radicals responsible for ozone formation. A daytime HONO source at the snow surface appears to be primarily responsible for the contribution of HONO to the radical pool. However, the magnitude of the contribution of HONO to the radical pool is uncertain at this time due to the limited vertical extent of HONO measurements made during the 2013 study. There are also questions about the accuracy of these measurements, which were made using a single method, resulting in a significant amount of uncertainty in modeling the chemistry of ozone formation.

b. Uncertainties remain regarding the likely impact of nitrogen oxides (NO_x) and, to a lesser extent, volatile organic compound (VOC) emission controls on ozone levels:
   i. Analysis of data from 2012 (when elevated ozone did not occur) suggests that the limited amount of ozone production that did occur was VOC limited, i.e., VOC reductions would produce ozone reductions whereas marginal NO_x reductions may result in increases in ozone. However, conditions with low ozone in 2012 cannot be used to predict ozone sensitivity to precursors during winter inversion conditions with snow cover, and further analysis is needed to assess ozone sensitivity during the 2013 episodes.
   ii. The effectiveness of NO_x controls will also be impacted by the extent to which unreactive NO_z species (including HNO_3 and organic nitrates) are being recycled back into reactive NO_x by heterogeneous chemistry in snow and on particulates. Details of these potential heterogeneous reactions are not yet understood well enough to be included in photochemical models needed for evaluation of control strategies.
   iii. Measurements made during 2013 suggest that VOC reactions in the snow may contribute to ozone chemistry within the layer of air just above the snow surface (the mixed layer). The potential implications of this finding on the efficacy of VOC and NO_x controls are not yet known and further study is needed.
   iv. Oxidation of VOCs is a key step in ozone accumulation. While the reactivity of VOCs varies widely, the relative contribution of individual VOC species to ozone formation depends on their abundance as well as their reactivity. Measurements made during 2012 and 2013 indicate that alkanes (including propane, iso- and n-butane and iso- and n-pentane), are much more abundant and as a result likely contribute more to ozone formation in the Basin than the more reactive but less abundant aromatic VOCs (including toluene and xylene). Nevertheless, small reductions in emissions of aromatics may be as effective as larger reductions in emissions of alkanes given the greater reactivity of aromatics. There do not appear to be large sources of other highly reactive VOCs (alkenes) in the Basin as alkene concentrations were very low relative to alkanes and aromatics.

IV. Emissions

a. Some important progress has been made on developing emission inventories for the Basin but the available data remain incomplete. Several groups, including the Utah Division of Air Quality, EPA Region VIII, and Federal Land Managers (through the Utah Air Resource Management Strategy project and the "3-States" and "West Jump" air quality modeling studies) are currently working on inventories for the Basin. Progress would be enhanced by more formal coordination of effort between these groups and the energy producers.

b. Field measurements of emissions from produced water ponds were conducted during the winter of 2012-2013 which showed that, while wintertime pond emissions comprise a small part of total VOC emissions in the Uinta Basin, VOC emitted from produced water ponds tend to be enriched in reactive VOC.
c. Field measurements made by the NOAA mobile laboratory during UBOS 2012 show significant differences in VOC emission composition depending on well and equipment types and are broadly consistent with VOC emission profiles applied to different source categories (venting, flashing, dehydrators, etc.) in the 2008 Western Regional Air Partnership (WRAP) inventory.
d. Obtaining comprehensive emissions data for the Basin is made difficult in part due to a mixture of private, federal, state and Indian surface and mineral rights ownership which results in complex regulatory jurisdictions and inconsistent reporting requirements.
e. Inventory data specific to the winter ozone season are needed as emissions from some types of sources (such as evaporation ponds and methanol use) have large seasonal variations.
f. Additional information is needed on sources of formaldehyde (which is a highly reactive volatile organic compound (VOC) that accelerates the formation of ozone), including methanol use and degree of contamination with formaldehyde and operation of dehydrators.
g. Important components of the inventory that need to be more carefully quantified include emissions of VOCs from oil, condensate and produced water storage tanks, as well as fugitive emissions from leaking components and other sources and from venting, blowdowns and other intermittent events.

V. Recommendations for Future Analyses

a. Additional field data collection and analysis are needed to improve our understanding of several key features of the winter episodes to the point where meteorological and photochemical models suitable for analyzing alternative regulatory scenarios can be developed. Two areas of particular importance were identified:
    i. The highest priority studies would focus on improved, more robust measurements of HONO concentrations and related species, their vertical distribution and temporal variations. The response of ozone to changes in VOC and NO_x emissions is highly sensitive to HONO, so a clear understanding of HONO formation and removal mechanisms is critical.
    ii. Development of a comprehensive and accurate winter emission inventory for the Basin suitable for modeling applications (i.e., including sufficient speciation of chemical compounds and spatial and temporal detail) remains a critical requirement. There is a need to prioritize and coordinate efforts among the various groups that are currently developing inventories. In addition, work on "top-down" evaluation of inventories using available air quality observations is needed.
b. Several other data collection and analysis needs were identified by the UBOS research team; these are described in Section 2.6.

VI. Implications for Control Strategies

a. Ozone levels in excess of the EPA 8-hour standard are only observed during winter inversion periods; ozone levels on the majority of days during the year are below the EPA standard and exceedances of the standard do not occur every year. This suggests that episodic or seasonal controls may be a useful component of an overall air quality management strategy for the Basin.
b. Emission reductions at the Bonanza power plant are unlikely to have any effect on winter ozone episodes.
c. Reductions in all VOC emissions will be beneficial; reductions in the more reactive VOC species, such as formaldehyde and aromatic VOC, will be more beneficial on a per ton basis but less reactive VOCs dominate emissions, and therefore ozone production, in the Basin. Glycol dehydrators and produced water are two important sources of aromatic VOC.
d. Ozone response to NO_x reductions is less certain. NO_x control strategies will tend to be less effective if unreactive NO_z is converted to reactive NO_x by heterogeneous chemistry on snow or particulates, e.g., the conversion of HNO_3 to HONO in snow.
e. Reducing formaldehyde would be an effective way to reduce ozone, but it is not clear at this time which sources of formaldehyde (direct emissions from fuel combustion and use of methanol contaminated with formaldehyde or secondary formation of formaldehyde from VOC precursors) are most important.
f. Uncertainty in HONO sources and source strength (direct emissions or secondary formation from nitrogen precursors via several potential reaction pathways) makes it difficult to predict how responsive ozone will be to reductions in VOC and NO_x emissions.

inversion is a very shallow layer with even higher levels of CH_4 and extremely high NO_2 with a significant dip in O_3 indicating titration by NO and conversion to NO_2. This is in contrast to profile 2 just to the west of the gas field (Figure 4-17) where a similar inversion structure has enhanced ozone but NO_2 levels are lower. Ozone below the inversion is also higher than in the gas field reaching ~100 ppb. Profile 3 to the NW of the gas field has a well-mixed layer below the inversion with O_3 of ~100 ppb again indicative of continuing O_3 production as precursors move out of the gas field.

Profiles on February 4 (not shown) have generally well-mixed conditions through a somewhat deeper boundary layer that extends up to 1800 masl in several profiles. For all six profiles on this day O_3 mixing ratios in the boundary layer are over 100 ppb. On February 5 the profiles all have well defined temperature inversion with a top at or just above 1600 masl (Figure 4-19). The trace constituents are well-mixed in the layer. Ozone is above 100 ppb, but somewhat different from the other days as O_3 is highest near the natural gas field exceeding 120 ppb (profiles 3 and 4). All the profiles show a gradual decrease of the trace gas measured concentrations including O_3 up to ~1850 masl. This layer above the lower sharp inversion layer is a characteristic in most of the profiles obtained by the aircraft and represents mixing out of the lowest surface layer into a gradient layer above.

4.4.3 Evidence of Bonanza Power Plant Plume in Vertical Profiles

Profile 4 on February 2 (Figure 4-17) and Profiles 1 and 3 on February 5 (Figure 4-19), as well as on February 4 (not shown), show clear evidence of a plume from the coal-fired Bonanza Power Plant, with enhancements in CO_2, CO, and NO_2 but with low CH_4 and a corresponding depletion in O_3. The power plant plumes were encountered in relatively close proximity to the power plant (~10-16 km). The low CH_4 along with lower O_3 are a clear indication that this plume did not originate from surface sources within the boundary layer. The depression of the O_3 mixing ratio below the tropospheric background measured outside the plume is a clear indication of O_3 titration by the power plant emitted NO. A buoyant plume of emissions from the power plant, whose stack height is at 182 m above ground level, or 1715 masl, is lofted above the 1600-1700 masl inversion layer, and remains above the inversion in a layer that varies in height between 1800 and 1950 masl. This is also shown in photographs taken from the aircraft during the campaign, which clearly show the buoyant plume from the plant above the hazy inversion layer below (Figure 4-20). We conclude that it is unlikely that the power plant emissions contributed significantly to the pollution observed at the surface during this strong temperature inversion event.

Figure 4-20. Photograph taken from the aircraft of the Bonanza Power Plant and its plume rising above the inversion layer on February 2, 2013.

4.5 Flask Samples from Aircraft

Discrete whole air samples were collected in glass flasks aboard the aircraft throughout the seven flights of 2013. Flask samples were also collected in the previous year, in February 2012. Here we present measurements of the whole air collected in flasks in both years, which were analyzed by NOAA's Global Monitoring Division (GMD) in Boulder, CO. In both years, flask samples were also measured at the University of Colorado's Institute of Arctic and Alpine Research (INSTAAR) for additional non-methane hydrocarbons (NMHC), and here we present a subset of that data from 2013. The locations of flask samples over the Uinta Basin in both years are shown in Figure 4-21, along with point sources of possible emissions and oil and gas wells. The 2013 flasks were preferentially sampled near Horsepool, while in 2012 more uniform sampling was achieved.

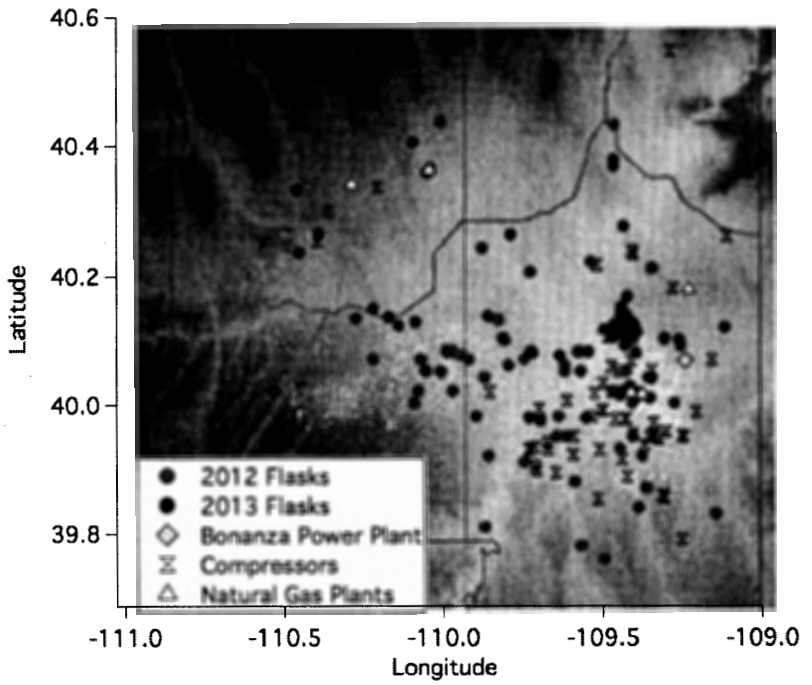

Figure 4-21. Location of flask samples collected in 2012 (red) and 2013 (blue) over the Uinta Basin. Gas wells are indicated in light blue and oil wells in green.

4.5.1 Comparison of Flask Sample Measurements in 2013 and 2012

Figure 4-22 (panels 1-5) shows the measurements of light hydrocarbons that are components of raw natural gas as they correlate with CH_4 in air samples collected in flasks aboard the aircraft in 2012 (gray) and 2013 (blue, red, yellow or green according to the location of the sample collection). Mole fractions of propane (C_3H_8), n-butane (n-C_4H_{10}), n-pentane (n-C_5H_{12}), isopentane (i-C_5H_{12}), and benzene (C_6H_6) show high correlation with CH_4 in both years. Figure 4-22 (bottom right panel) also shows the relationship between CO and CH_4 measured in flask samples in each year; these gases are less well correlated, as discussed in the previous section for the continuous data. As seen in the continuous data (Figure 4-5), CO is more enhanced per unit CH_4 in the SW quadrant of the basin (green). Figure 4-23 shows 2013 measurements of several additional hydrocarbons in the same flasks (from University of Colorado's INSTAAR), all showing correlation with CH_4 and significant enhancements. Some hydrocarbons show higher enhancements per unit CH_4 in the NW and SW quadrants (green and yellow), over the oil field, than in the NE and NW (red and blue), over the gas field. All species were present in significantly higher concentrations in 2013 compared with 2012, most likely because of the shallow layer in which emissions were trapped in 2013 and the lack of winds flushing the basin. In 2012, boundary layer heights were between 500 and 1000 m above ground level during the campaign, while in 2013 the emissions were trapped in a boundary layer of only 100-300 meters.

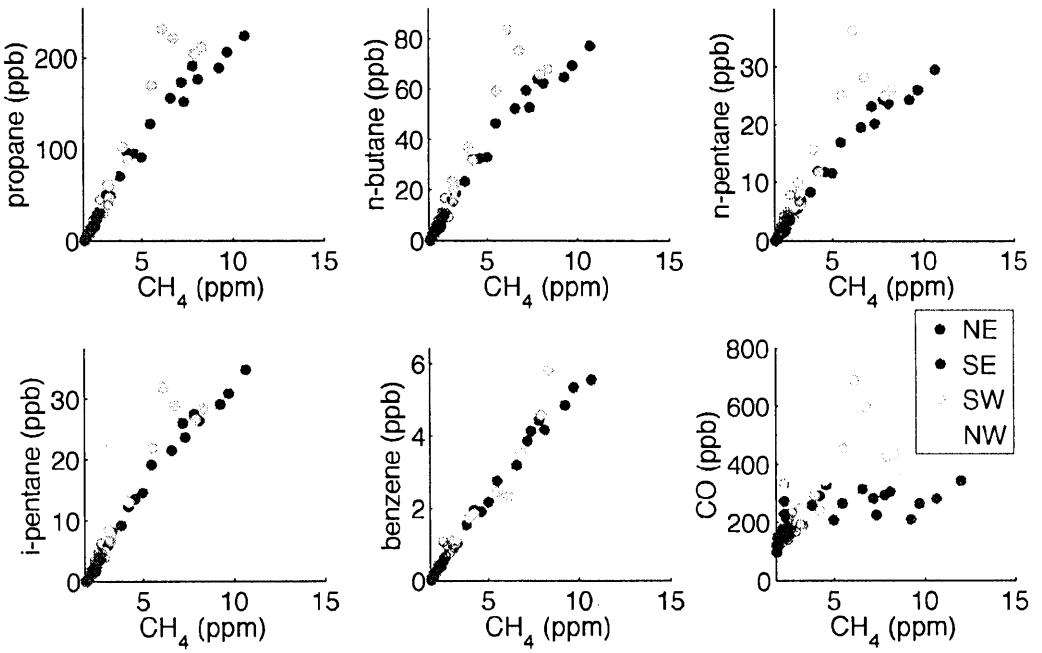

Figure 4-22. Measurements of light hydrocarbons (first five panels) and CO (bottom right) plotted against CH_4 mole fraction from air samples collected in flasks over the Uinta Basin in 2013 (blue, red, green or yellow based on quadrant) and 2012 (gray). All data from NOAA/GMD.

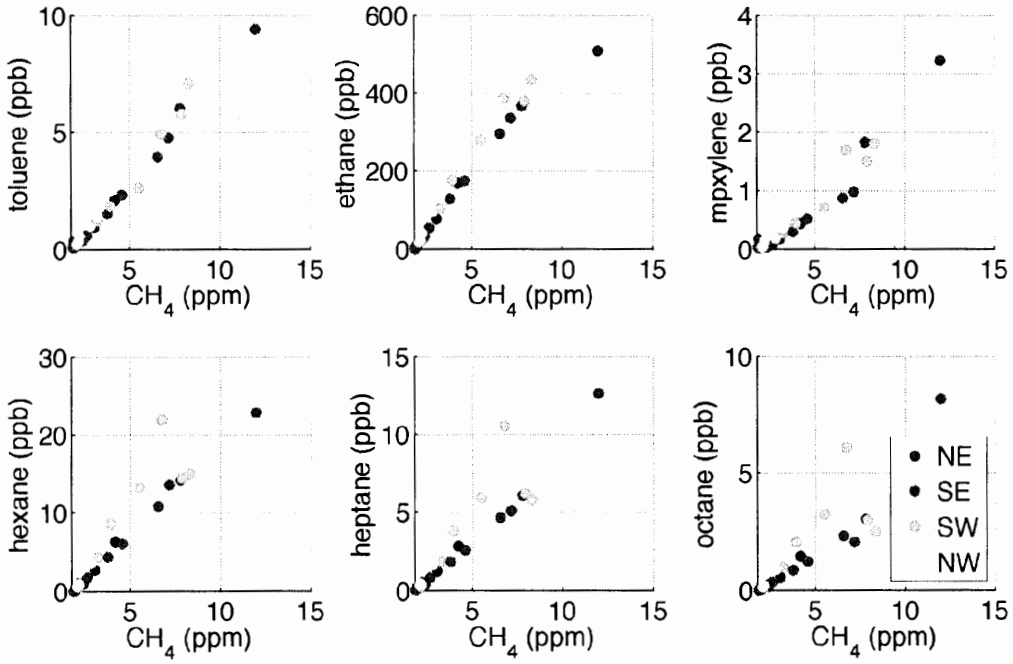

Figure 4-23. Measurements of heavier hydrocarbons in flasks collected aboard the aircraft, January 31 - February 7, 2013, colored by quadrant (CH_4 from NOAA/GMD and NMHC from CU INSTAAR).

4.6 Conclusions

Continuous measurements of O_3, CH_4, CO, CO_2, and NO_2 along with periodic flask measurements during seven aircraft flights between January 31 and February 7, 2013 present an unprecedented picture of both the horizontal and vertical distribution of key atmospheric constituents across the Uinta Basin. With optimal conditions for enhanced O_3 production during the winter of 2013, the relationship between precursor emission sources and O_3 production across the basin was established. Highest concentrations of CH_4 and related non-methane hydrocarbons and NO_2 were observed over the natural gas field in the SE portion of the basin. Longer-lived gases such as CH_4, CO, and CO_2 were more uniformly dispersed across most of the basin and were significantly elevated above background levels. These results suggest that the natural gas field is the likely primary source of O_3 precursor emissions. High O_3 mixing ratios were often seen well away from the gas field itself, strongly indicating ongoing photochemical production as precursors are dispersed across the basin. The strongest enhancements were seen in a relatively shallow surface layer with a strong temperature inversion with a top near 1650±50 masl. There was a gradient layer above this inversion with elevated constituent mixing ratios that gradually declined to near tropospheric background values between 1800 – 1900 masl. Even in the SW sector (over the oil production field), where very high CO values were found on all flights, O_3 was not higher than in other locations. O_3 was

positively correlated with CO over the Basin (Figure 4-11) as might be expected when the CO source is associated with combustion where NO, a primary O_3 precursor, is also emitted. In the SW sector, however, high NO_2 was not generally measured with the very high CO found in this sector and there was no indication of additional O_3 formation.

The highest values of CO measured during the flights were in the SW sector over the region of oil production in Duchesne County. No other constituents measured in this sector showed values elevated above those seen in other parts of the basin. In particular, there was no indication of additional O_3 production seen in conjunction with these very high CO values. Neither high CO_2 nor NO_2 values accompanied these high CO amounts. Correlation plots between CO and other constituents often showed a much different relationship in the SW quadrant, over the oil field, than seen in the other portions of the basin. No immediate source was identified for the strong CO emissions, but the signature of a high CO to CO_2 enhancement ratio indicates a source with inefficient combustion, possibly from the pump jack engines operating in the oil field.

A number of profiles in relatively close proximity (~16 km) to the Bonanza power plant encountered a layer of enhanced CO, CO_2 and NO_2 but with no enhancement in CH_4 and slightly depleted O_3 at an altitude of 1800 – 1900 masl. This composition of trace gas levels was a clear indication of transit through the Bonanza power plant plume. Visual identification of the plume, the altitude of the plume based on the stack height and plume rise, and its composition were clear indicators that the plume had risen through the strong inversion layer. There was also no sign of mixing of the plume from above the inversion back downward to the surface where it could contribute to O_3 production within the geographical boundaries of the study .

4.7 References

Bishop, G. A., and D. H. Stedman, 2008. A decade of on-road emissions measurements, *Environmental Science & Technology*, *42*(5), 1651-1656.

Karion, A., C. Sweeney, S. Wolter, T. Newberger, H. Chen, A. Andrews, J. Kofler, D. Neff, and P. Tans, 2013. Long-term greenhouse gas measurements from aircraft, *Atmos. Meas. Tech.*, *6*(3), 511-526.

Miller, J. B., et al., 2012. Linking emissions of fossil fuel CO_2 and other anthropogenic trace gases using atmospheric (CO_2)-C-14, *J. Geophys. Res.-Atmos.*, *117*.

Peischl, J., et al., 2013. Quantifying sources of methane using light alkanes in the Los Angeles basin, California, *Journal of Geophysical Research: Atmospheres*, n/a-n/a.

Turnbull, J. C., et al., 2011. Assessment of fossil fuel carbon dioxide and other anthropogenic trace gas emissions from airborne measurements over Sacramento, California in spring 2009, *Atmos. Chem. Phys.*, *11*(2), 705-721.

Wunch, D., P. O. Wennberg, G. C. Toon, G. Keppel-Aleks, and Y. G. Yavin, 2009. Emissions of greenhouse gases from a North American megacity, *Geophys. Res. Lett.*, *36*, 5.

5.3.9 Lidar Measurements

5.3.9.1 Meteorological Processes in the Atmospheric Boundary Layer Using Doppler Lidar

Concentrations of pollutants (including ozone O_3, methane CH_4, ethane C_2H_6, etc.) are determined by emission rates and chemical transformations over a time period, by the 3-D volume occupied by those pollutants, by how well they are mixed within the volume, and by the time constants for mixing out of that volume. The volume is determined by the vertical depth and horizontal extent of distribution of the pollutants. In general, stable, light-wind, cold-surface wintertime conditions are characterized by inhibited mixing, and consequently trapping of surface-emitted species in shallow, ground-based layers, inhomogeneous or "lumpy" concentrations in the horizontal, and layered structure in the vertical.

Instrumentation was deployed to the Uinta Basin during January and February 2013 to study meteorological processes controlling the extent and transport of pollutant species in the horizontal and vertical, and their vertical distribution. Tethered balloons and ozonesondes (to measure profiles of O_3 and of atmospheric thermodynamic variables), instrumented light aircraft and mobile vans, and an O_3-profiling differential-absorption lidar (DIAL) system are described elsewhere in this report. A Doppler lidar system, NOAA's High Resolution Doppler Lidar (HRDL), described by Grund et al. (2001), was deployed to the Horse Pool site to measure flow properties at high resolution and precision in the lowest 2 km of the atmosphere; this site was in the eastern sector of the Basin. Such high resolution and precision was needed to sample the weak and often shallow flow layers affecting the horizontal and vertical distribution of atmospheric contaminants.

Within the Uinta Basin, mobile van and light aircraft measurements found source activity to be highly variable in the horizontal, as described elsewhere in this report. For example, gas-drilling operations predominantly in the eastern sector of the Basin resulted in higher concentrations of CH_4 and other substances, predominant oil extraction in the western sector produced a different mix of airborne chemicals, and significant NO_X emissions were localized in the south-central portion of the Basin near the Chapita site and other places (Figure 4-21). Such spatial source variability means that horizontal transport may play a role in the generation of secondary pollutants by mingling emissions from different source regions. So an important question is whether the weak flows in the Basin could perform this kind of transport in the strongly stable, light-wind wintertime conditions encountered during the high-O_3 episodes.

Flow in complex terrain is generally closely related to the topography. Figure 5-42 is a topographic map of the Basin with contours chosen to emphasize basin characteristics—the 1564-m contour between purple and blue represents the elevation of the Horse Pool site, and all elevations above 2164 m appear black, thus clearly outlining the Basin. It is of interest that, although the main drainage of the Uinta Basin is the northeast-southwest-flowing Green River, the Basin orientation is elongated west-east, the Green River marking the mid-basin low point.

Time-height cross sections of HRDL-measured wind profiles for a 24-hr diurnal period are shown in Figure 5-43 for 15 Feb 2013, a day on which 8-hour average ozone concentrations at Horse Pool reached 123 ppb. During nighttime hours the near-surface winds blew from an

easterly direction, but during the day they reversed to westerly. Wind speeds were very weak at 1-2 m s^{-1}. The diurnal cycle was clear on this day; on other days this tendency was also observed, although passing synoptic scale disturbances often interrupted the pattern, because the diurnal flows were so weak.

Diurnal cycles of winds in complex terrain are generally driven by the daily heating and cooling cycle at the surface. Over snow-covered surfaces at night, strong cooling occurs which drives shallow downslope drainage flows. On the scale of the Basin, this drainage flow would be from easterly directions at Horse Pool. Daytime westerly flows could be a result of daytime surface heating but this is less certain given the cold temperatures, strong stability, and snow surface. Westerly flow in this part of the Basin would be consistent with a thermally forced, up-basin wind due to surface heating. Instrumented tower data at Horse Pool provides evidence for surface heating in the form of temperature traces at 2, 9, and 18 m above ground, which show the lower-level temperatures much colder at night than higher up, but which crossed over during the morning hours to become 1-2 degrees warmer at the lower levels (Figure 5-44). Positive near-surface heat fluxes, indicative of surface heating, were also evident during the day.

When the surface is warm relative to the adjacent atmosphere, an unstable boundary layer or 'mixed layer,' sometimes referred to as a convective boundary layer (CBL), can form. A signature of a CBL is that the potential temperature profile $\theta(z)$ is approximately constant or slightly decreasing with height, and the profiles of other constituents, such as water vapor, O_3, CH_4, etc., may also become constant or nearly constant with height. Figure 5-45 shows θ and O_3 profiles from a tethered-balloon system at Horse Pool for 1409 MST (2109 UTC) on 14 Feb. The nearly constant profiles and warm surface indicate a mixed-layer structure. For boundary layers in general, a mixed-layer structure can be produced by wind shear in addition to surface heating, but here the wind speeds, and therefore the shear, are too weak to contribute significantly to the mixing through the CBL. Existence of CBL structure under these conditions is thus another indicator of surface-based heating of the atmosphere.

As discussed in Section 3, high-O_3 events coincided with the development of a strong pool of cold air in the Basin. During winter, cold air accumulates in the bottom of the Basin at night but is not mixed out during the day due to relatively weak surface heating consistent with low sun angles, highly reflective snow cover, and short days. The resulting pool of cold air builds in depth and strength, persisting through many days until the process is interrupted by a change in the synoptic pattern (e.g., [*Whiteman et al.*, 1999]) . The cold-air inversion layer, comprising this cold pool, suppresses mixing, so at night, the cold surface generates drainage flows that carry surface-released pollutants to lower regions of the Basin with little vertical mixing. During the day, the warm-surface-based CBL mixes near-surface pollutants upward through the shallow mixed layer, and the daytime flow carries the polluted layer up slope. At Horse Pool, the nocturnal flows were seen to be from an easterly direction, and the daytime up-basin flows, from a westerly direction. Also at the Horse Pool site, Figure 5-45 shows that the CBL only grew to a depth of ~70 m during the day.

Tethered-balloon soundings were taken simultaneously at two other sites in the Uinta Basin, at Ouray low in the Green River Valley (elevation 1430 m) and at Fantasy Canyon (elevation 1470 m) to the south-southeast of Horse Pool at an elevation intermediate between the other two sites (Figure 8-6). Figure 5-46 shows afternoon profiles of θ and O_3 at all three sites. A mixed-layer structure was evident at all sites, but the CBL was deepest at the lowest site (Ouray), and shallowest at the highest of the three sites (Horse Pool). Significantly, when plotted against height above sea level (ASL) as the vertical coordinate, the height of the CBL was very similar at about 1650 m ASL at all sites. The top of the inversion layer, marking the top of the cold pool, was also similar at ~1900 m, a value seen on other mid to late episode days. In other words, the cold pool was essentially a lake of cold air filling the Basin and having a relatively flat, level top, as is often evident when fog or stratus clouds occupy the cold pool. In addition, the afternoon mixed layer also tended to have a level top, even though the Basin topography rises and falls beneath it.

Interesting questions are, how do the cold-pool and mixed-layer structure evolve as an episode builds, and is the inversion at the top of the cold pool impenetrable or leaky? Figure 5-47a shows the afternoon vertical structure at the three sites at the beginning of an episode on 1 February, and Figure 5-47b shows mid-episode afternoon profiles four days later on 5 February. The θ profiles on 1 Feb show that the surface-based inversion at the top of the cold pool reached just over 1750 m ASL. As the episode proceeded, the cold pool depth grew to nearly 1950 m by 5 Feb. The afternoon CBL or mixed-layer height, however, remained the same at just under 1650 m ASL as seen in both the θ and O_3 profiles. Inversion strengths above the mixed layer of 4°/100 m (1800-1900 m on 5 Feb) to 6°/100 m (1650-1750 m on 1 Feb) represent very strong inversions, which should strongly inhibit vertical displacement and mixing into the inversion layer.

The depth of the shallow mixed layer changed little through the episode, but the layer cooled by 2°C and the O_3 produced from concentrated pollutants, which were emitted into and then trapped within this layer, increased by ~40 ppb over the 5-day period (Figure 5-47-left panels). Above the cold-pool inversion on 1 Feb, O_3 concentrations were ~50 ppb, which coincided with background values measured during the previous basin clean-out period (29 January) and at rural sites in Utah, such as Canyonlands NP. These low concentrations are seen above 1750 m MSL, corresponding to the cold-pool top. Just below the top of the cold pool, O_3 concentrations were significantly above background, indicating that "leakage" of pollutants upward into the strong inversion layer has occurred, most likely as a result of complex flow interactions within the Basin cold pool, as opposed to direct diffusion up through the inversion. This upward displacement of pollutants continued through the episode, as O_3 concentrations on 5 Feb exceeded 90 ppb below 1850 m and were well above background up to the top of the cold pool at 1900 m MSL. Such upward escape of pollutants into the inversion layer would have to be accounted for in performing basin-wide pollutant budgets.

Concentrations of many pollutants besides O_3 were found to be very high, even when compared with highly polluted urban areas, most notably ethane (Section 6.0). The vertical trapping of pollutants within the Basin by the cold-air inversion layer is a major factor, but the

light-and-variable nature of the winds also contributed. Light winds allow for large doses of emissions into an atmospheric volume as it passes over a source, and the variable winds allow the volume to pass over many sources, sometimes back and forth over a source region. The displacement of a small volume or "parcel" of air can be traced by calculating and plotting layer-averaged trajectories from the 20-min wind profiles (e.g., Figs. 5-2 and 5-43). For flows exhibiting a diurnal cycle, Allwine and Whiteman (1994) have argued that the net trajectory displacement over a 24-hr period is a measure of a "ventilation" effect of these flows. Measured trajectories have been used in prior studies to determine overnight transport of O_3 plumes [*Banta et al.*, 1998] and the effects of sea-breeze wind reversals on pollutant transport [*Banta et al.*, 2004; *Banta et al.*, 2011]. Here we use 24-hr forward trajectories to investigate transport and ventilation effects in the Basin.

Examples of 24-hr trajectories calculated from 20-min HRDL winds are given in Figure 5-48 for 30-31 Jan and 14 Feb., starting at about sunset (1700 MST or 0000 UTC). It is important to note that these are single-station trajectories, and the locations of the endpoints in time assumes that the winds over the relevant portions of the Basin are uniform, which is unlikely, especially as the trajectory height is closer to the ground and the location moves farther from the Horse Pool measurement site. The trajectories should be viewed as an indicator of the potential for transport and redistribution.

On 30 January (Figure 5-48a) the easterly drift of the low-level trajectories (black, red) early in the evening (closest to the measurement site) reflect the continuation of the daytime westerly-component flow. This flow reversed to the easterly drainage direction after 2100 MST (0400 UTC; see Figure 5-2). Over the next 9 hr the trajectory traveled more than 70 km to the west, until predawn and daytime flow became more variable and light. Another day showing large trajectory displacements was 31 January (Figure 5-48b). On both days O_3 concentrations were less than 80 ppb. In contrast, 14 February was one of the highest pollution days, ozone concentrations exceeding 140 ppb at the Ouray UDEQ monitoring site. Figure 5-48c shows that the 24-hr trajectory displacements below 200 m AGL were ~30 km or less indicating low ventilation factor. The weak, variable winds caused the trajectories to wander about within ~20 km of their origin, accumulating emissions from many sources—and presumably many *types* of source—in this area. The fact that the trajectories maintained direction for a few to several hours—in drainage or upslope flows, for example—means that transport of a few tens of km could occur, even though the winds were light. These distances would be sufficient to expose a traveling volume of air to several types of source within the Basin. In the western part of the Basin, where many sources are above the top of the high-pollution layer coinciding with the daytime mixed-layer (1650 m ±50 m), persistent downslope drainage flows are a potential mechanism for bringing emissions down into the lower levels of the Basin.

Another way to use wind data to trace air movement is backward trajectories, which are constructed by starting at a desired time and height, and using the observed winds to trace air-parcel locations backwards in time. Backward trajectories are useful for inferring potential sources for events occurring at a site. For example, on several occasions, anomalously low ozone concentrations were noted at 300-350 m above the Horse Pool site as described in

Section 8 and also shown in the TOPAZ lidar results below. Figure 5-49 shows backward trajectories for 300 m above Horse Pool passing over the Bonanza Power Plant power plant for one such occurrence. The trajectories passing over the power plant indicates that the O_3 "hole" was likely caused by titration of O_3 by NO emissions from the plant, as described in the section on TOPAZ results below. In particular, 14 Feb was a day exhibiting high ground-level O_3 concentrations at sites within the Basin, but the Bonanza Power Plant effluent plume was *above* the cold-pool inversion and thus completely isolated from the near-surface pollutant layer, at the short time scales involved in the transport of the plume across the Basin. This further illustrates that the Bonanza Power Plant power plant plume did not contribute to the high ground-level O_3 during the highest wintertime O_3 events.

5.3.9.2 TOPAZ Lidar

The primary objective of deploying the TOPAZ lidar at the UBOS studies was to characterize the vertical structure of ozone from near the surface to a few kilometers AGL at high temporal and spatial resolutions. In the lowest few hundred meters, the TOPAZ ozone profiles complemented the collocated ozone tether sonde measurements at Horse Pool by providing temporal continuity between tether sonde launches. The lidar ozone profile measurements above 500 m AGL provided information about the ozone structure beyond the maximum altitude reachable with the tether sondes. This was critical for detecting ozone layers aloft, which may be associated with long-range transport of ozone in the lower free troposphere or downward mixing of stratospheric ozone. Under the right conditions, these ozone layers aloft can be mixed down to the surface and can impact surface ozone concentrations. One hypothesis that had been put forth prior to the UBOS studies was that the high surface ozone concentrations often observed during the winter months in the Uinta Basin were at least partly caused by long-range or stratosphere-to-troposphere transport of ozone. The ozone lidar observations were crucial for confirming or disproving this hypothesis. During the two UBOS studies, numerous comparisons were performed between the lidar measurements and observations from the tethered ozone sondes, the surface in situ ozone sensors, and the free-flying ozone sondes (2012). Generally, the lidar measurements compared well with the other ozone measurements, and the observed discrepancies were within the stated instrument accuracies of the lidar and the in situ sensors.

UBOS 2012

The TOPAZ ozone lidar was operated on 14 days between 3 and 29 February 2012 and recorded 62 hours of ozone and aerosol backscatter profile data. In the absence of any high ozone events, the sampling strategy consisted of operating TOPAZ for several hours at a time and covering different segments of the diurnal cycle on different days. TOPAZ ozone data are posted at http://www.esrl.noaa.gov/csd/groups/csd3/measurements/ubwos/topaz/. Figure 5-50 shows a 5-minute average ozone profile observed in the early afternoon on 7 February 2012. This ozone profile was typical for the vertical ozone structure observed during UBOS 2012, which was characterized by unusually warm and snow-free conditions, and fairly deep, well-mixed boundary layers. Figure 5-50 also illustrates how the lidar ozone observations from three elevation angles were spliced together to create a composite vertical profile extending from 15 m to about 3 km AGL.

Figure 5-51 shows all ozone lidar measurements from the 2012 study displayed as normalized probability distribution functions (PDFs) for three altitude ranges: 15 – 200 m AGL, 200 – 1000 m AGL, and 1000 – 3000 m AGL. The mean ozone values for these altitude ranges were approximately 46 ppbv, 48 ppbv, and 52 ppbv, respectively. Figure 5-51 shows that no ozone values above about 75 ppbv were measured with the lidar at any altitude below 3000 m AGL. In particular, no exceedances of the 8-hour National Ambient Air Quality Standard were observed. This lack of high ozone episodes was likely due to the fact that the boundary layer was generally rather deep and well-mixed, which prevented a buildup of high concentrations of ozone and its precursors. The almost complete absence of any snow cover during the UBOS 2012 study prevented the formation of a shallow cold-air pool and the development of strong temperature inversions. As a result, the boundary layer was much deeper and much better ventilated than during typical wintertime conditions in the Uinta Basin. Figure 5-51 also reveals that on average ozone concentrations were increasing slightly with altitude during UBOS 2012. The mean ozone value of about 52 ppbv in the upper altitude bin is typical for background ozone conditions in the lower free troposphere for the western US. The slightly lower ozone values in the two altitude ranges below 1000 m are probably due to titration and surface deposition of ozone. The slight vertical gradient of ozone and the similarity of the ozone PDFs for the three altitude ranges are consistent with the generally well-mixed conditions observed during UBOS 2012.

A few times during the 2012 study, very low ozone values due to titration were observed with the in situ sensors at the Horse Pool site. TOPAZ showed that these low ozone values extended to several hundred meters AGL throughout the well-mixed BL. A trajectory analysis using HRDL lidar wind observations indicated that in these cases the Bonanza Power Plant power plant plume was advected to the Horse Pool site, thus linking the observed ozone titration to the NOx-rich power plant plume.

UBOS 2013

TOPAZ was operated on 22 days between 22 January and 18 February 2013 and recorded approximately 230 hours of ozone and aerosol backscatter profile data. Data were collected during most of the diurnal cycle. The ozone and aerosol profiles typically extended up to 2.5 km AGL, except when low clouds were present, which restricted the maximum range of the lidar to the base of the clouds. The lidar was not operated during periods of precipitation and fog. TOPAZ ozone data are posted at http://www.esrl.noaa.gov/csd/groups/csd3/measurements/ubwos13/topaz/. Figure 5-52 gives an overview of all ozone profiles measured during UBOS 2013. Ozone profiles are only shown up to 1000 m AGL to depict the details of the ozone structure in the lowest few hundred meters. Strong lidar signal attenuation due to the high ozone and aerosol concentrations observed in 2013 resulted in small gaps in the spliced ozone (and aerosol backscatter) profiles, shown as white horizontal bars in Figure 5-52. TOPAZ captured the evolution of several high ozone episodes, including their multi-day buildup followed by a partial or complete cleanout of the Uinta Basin due to passing synoptic scale storms. Two complete episodes during the first half of February, the last couple of days of the late January episode, and the first day of ozone buildup starting on 18 February were captured. No data were taken during the 27 January and 8-11 February storms, which were accompanied by precipitation and low clouds. However,

TOPAZ documented the cleanout by a dry cold front on 17 February followed by a quick rebound in ozone (albeit in a very shallow layer) on the next day (see bottom panel of Figure 5-52). From 1 – 7 February, thick fog occurred at the Horse Pool site at night and in the morning, which limited the times when the lidar could be operated.

In contrast to 2012, winter weather conditions during 2013 in the Uinta Basin were more typical, with snow-covered ground and a persistent, shallow cold-pool layer. The strong inversion capping the cold-pool layer coupled with very light boundary layer (BL) winds caused a buildup of pollutants at the Horse Pool site, which after several days led to very high afternoon ozone concentrations of 120 to 150 ppbv. The high ozone episodes came to an end when high winds and strong mixing associated with the storm systems on 27 January, 8 February and 17 February diluted and flushed out the high ozone concentrations. Figure 5-53 shows the time-height cross section of ozone mixing ratio measured with TOPAZ on 17 February when a dry cold front passed over the Horse Pool site around 18:30 MST. This figure also shows the horizontal wind speed and direction profiles observed with the HRDL lidar, which are depicted as wind barbs, color-coded according to wind speed. Strong westerly winds were present above 400 m AGL in the afternoon, which dropped down to the surface in the wake of the passing cold front. As a result, the pollutants in the BL were flushed out and near-surface ozone concentrations dropped from about 130 ppbv to around 50 ppbv in less than one hour. The in situ surface ozone observations from the TECO and NOx cavity ring down instruments at Horse Pool also show this precipitous decrease in ozone.

Figure 5-54 shows 15-minute average ozone profiles for each day TOPAZ was operational. The profiles were observed when BL ozone peaked in the afternoon and are grouped by ozone episode. Despite the snow cover and cold temperatures, the TOPAZ observations show well-mixed ozone profiles up to about 100 m AGL. After several days of pollutant buildup, BL ozone values reached 120-150 ppbv. Above the mixed layer, ozone values gradually decreased to tropospheric background values of around 50 ppbv throughout the several-hundred-meter-deep cold-pool layer and then stayed constant above that up to about 3 km AGL. During the ozone episodes, the lidar observations show no indication of either vertical or horizontal transport of high ozone levels to the surface. This disproves the hypothesis that transport of ozone from outside the Uinta Basin contributes in a significant way to the wintertime high ozone episodes and instead supports the notion that ozone is locally produced in the Uinta Basin.

Just as in 2012, TOPAZ occasionally observed ozone titration as the NOx-rich plume from the nearby Bonanza Power Plant power plant was advected over the Horse Pool site. As an example, Figure 5-55 shows a two-hour time-height cross section from near the surface to 600 m AGL measured with TOPAZ in the evening of 14 February with the coincident ozone tether sonde measurements overlaid. Both lidar and ozone sonde show ozone values below 30 ppbv between 300 and 400 m AGL during a 30-minute period. Contrary to 2012, low ozone values were confined to the upper part of the cold-pool layer above the BL. This suggests that power plant NOx was very likely not part of the precursor mix that led to the high surface ozone values observed in 2013.